JGR Biogeosciences

RESEARCH ARTICLE
10.1029/2019JG005082

Special Section:
The Energy Exascale Earth System Model (E3SM)

The Effects of Phosphorus Cycle Dynamics on Carbon Sources and Sinks in the Amazon Region: A Modeling Study Using ELM v1

Xiaojuan Yang[1], Daniel M. Ricciuto[1], Peter E. Thornton[1], Xiaoying Shi[1], Min Xu[2], Forrest Hoffman[2], and Richard J. Norby[1]

[1]Environmental Sciences Division, Oak Ridge National Laboratory, Oak Ridge, TN, USA, [2]Computational Sciences & Engineering Division, Oak Ridge National Laboratory, Oak Ridge, TN, USA

Key Points:
- We implemented a prognostic phosphorus cycle and carbon-nitrogen-phosphorus interactions into ELM v1
- ELM v1 simulations show phosphorus cycle dynamics affect both sources and sinks of carbon in the Amazon region
- The effects of P limitation would become increasingly important as CO_2 increases in the future

Correspondence to:
X. Yang,
yangx2@ornl.gov

Citation:
Yang, X., Ricciuto, D. M., Thornton, P. E., Shi, X., Xu, M., Hoffman, F., & Norby, R. J. (2019). The effects of phosphorus cycle dynamics on carbon sources and sinks in the Amazon region: a modeling study using ELM v1. *Journal of Geophysical Research: Biogeosciences*, *124*, 3686–3698. https://doi.org/10.1029/2019JG005082

Received 8 FEB 2019
Accepted 25 SEP 2019
Accepted article online 15 OCT 2019
Published online 4 DEC 2019

Abstract Tropical forests play a crucial role in the global carbon cycle, accounting for one third of the global net primary productivity and containing about 25% of global vegetation biomass and soil carbon. This is particularly true for tropical forests in the Amazon region, as these comprise approximately 50% of the world's tropical forests. It is therefore important for us to understand and represent the processes that determine the fluxes and storage of carbon in these forests. In this study, we show that the implementation of phosphorus (P) cycle and P limitation in the version 1 of the Energy Exascale Earth System Model land model (ELM v1) improves simulated spatial pattern of wood productivity. The P-enabled ELM v1 is able to capture the declining west-to-east gradient of productivity, consistent with field observations. We also show that by improving the representation of mortality processes using soils data, ELMv1 is able to reproduce the observed spatial pattern of above ground biomass. Our model simulations show that the consideration of P availability leads to a smaller carbon sink associated with CO_2 fertilization effect and lower carbon emissions due to land use and land cover change. Our simulations suggest P limitation would significantly reduce the carbon sink associated with CO_2 fertilization effects through the 21st century. We conclude that P cycle dynamics affect both sources and sinks of carbon in the Amazon region, and the effects of P limitation would become increasingly important as CO_2 increases. Therefore, P limitation must be considered for projecting future carbon dynamics in tropical ecosystems.

1. Introduction

Tropical forests play a crucial role in the global carbon (C) cycle, accounting for roughly one third of the global net primary productivity (NPP) and containing about 25% of global vegetation biomass and soil C (Pan et al., 2011). This is particularly true for tropical forests in the Amazon region, as they comprise approximately 50% of the world's tropical forests (Castanho et al., 2013; Pan et al., 2011). However, there is a lack of agreement on their contribution to the global C balance due to large uncertainties associated with the sources and sinks of C in the Amazon region (Mitchard, 2018).

It has been generally agreed that undisturbed rainforests in the Amazon region act as a C sink (Brienen et al., 2015; Pan et al., 2011), although the size, causes, and the future trend of the sink are quite uncertain (Mitchard, 2018). A recent field study by Brienen et al. (2015) suggested that the land C sink in the intact Amazon forests is becoming saturated. The exact causes of this saturation are unknown. Hedin (2015) suggested that increased nutrient limitation might be one of the reasons for the land C sink saturation. Changes in climate might also be a contributing factor. Clark et al. (2013) found that climate-driven declines in productivity exceeded the positive response associated with increasing atmospheric CO_2. Tropical forests have also acted as an important source of C as a result of deforestation associated with land use and land cover change (LULCC). Deforestation affects very large areas of the Amazon forest; about 50 Mha was deforested between 2010–2012, mainly driven by clearing land for cropland or pastureland (Mitchard, 2018). Large uncertainties exist regarding the estimate of amount of C released from deforestation because of potentially large biases in the assumed distribution of vegetation biomass (Avitabile et al., 2016; Baccini et al., 2012; Mitchard, 2018; Mitchard et al., 2014). Previous studies suggested that as much as 60% of the total uncertainty in estimated emissions in Amazonia can be attributed to uncertainty in the vegetation C stocks (Houghton et al., 2000).

Spatially explicit ecosystem modeling has been used extensively to assess how the sources and sinks of C in the Amazon region respond to changes in atmospheric CO_2 and climate and land use change (Castanho et al., 2016; Galbraith et al., 2010; Huntingford et al., 2013; Rammig et al., 2010; Tian et al., 1998; Zhang et al., 2015). However, none of these modeling studies considered the effect of phosphorus (P) limitation and the interactions between P dynamics and C cycle responses to atmospheric CO_2, climate, and land use. P is generally considered as the most limiting nutrient in the old-growth, lowland tropical forests, as most soil P has been lost through weathering and leaching during millions years of soil development (Walker & Syers, 1976). Most of the P in tropical soils is either in organic form or in occluded form, with high recycling of P in tropical forests (Yang & Post, 2011). Wieder et al. (2015) evaluated how simulated CO_2 fertilization effects in Coupled Model Intercomparison Project phase 5 models could be constrained by nutrient availability and highlighted the importance of P limitation in constraining future NPP, especially in tropical ecosystems. Sun et al. (2017) also diagnosed P demand from ESMs and actual P availability and found that the extent of P deficit depends mainly on the assumptions about the availability of different soil P forms and called for more models to incorporate the P cycle and its interactions with the cycles of C and nitrogen (N). In recent years, increasing numbers of land surface models are incorporating P cycling, and carbon-nitrogen-phosphorus (CNP) interactions and model simulations from these P-enabled models have demonstrated that P limitation could constrain tropical ecosystem responses to CO_2, although the extent of P limitation remain uncertain (Goll et al., 2012; Wang et al., 2010; Yang et al., 2014; Yang et al., 2016).

There are increasingly more field observations of wood productivity and biomass available, in particular from the RAINFOR plots (http://www.rainfor.org), both in terms of temporal and spatial coverage. However, they are little used for the improvement of parameterization or process representation in tropical modeling studies, except for Castanho et al. (2013). Recent efforts utilizing these observational data were mostly focused only on the evaluation of a few dynamic global vegetation models (Castanho et al., 2016; Delbart et al., 2010; Johnson et al., 2016). Observational studies from RAINFOR plots provide important information about the distributions of forest productivity and aboveground biomass (AGB). For example, there are opposing west-east gradients of productivity and AGB in Amazon forests (Malhi et al., 2004; Malhi et al., 2009; Quesada et al., 2012). Productivity tends to decrease from west to east, whereas AGB tends to increase from west to east across the Amazon basin (Aragão et al., 2009; Quesada et al., 2009). These field observations also yield insights about the processes that drive the spatial variation of productivity and biomass. Quesada et al. (2012) found that the decreasing west-east gradient in productivity is mostly related to total soil P and the increasing gradient in AGB tends to be related to soil physical properties, rather than climate variations. Galbraith et al. (2013) suggested that mortality rate varied almost six-fold among tropical forest plots and generally depended on soil weathering stages. Integrating these field observational data and the associated process understanding into models should help us better quantify the C balance in the Amazon region and improve the predictive capability of models.

In this study, we explored the contributions of increasing atmospheric CO_2, climate, and LULCC to the C sources and sinks in the Amazon region. In particular, we investigated how the P cycle affects the magnitude and distribution of the C sources and sinks. We conducted the evaluation using the Energy Exascale Earth System Model (E3SM) land model (ELM v1). We used forest plot data to improve the parameterization and representation of key processes that control C fluxes and stocks in the tropical ecosystems. We performed a series of simulations to assess the C fluxes associated with CO_2, climate, and LULCC, with and without considering the P cycle. We examined the spatial and temporal patterns of C uptake and release by ecosystems in the Amazon region aiming to understand how P cycle processes influence these patterns.

2. Method

2.1. ELM v1

ELM v1 used in this study contains a number of improvements from ELM v0 (Ricciuto et al., 2018), which branched from community land model 4.5 (Oleson et al., 2013) that included vertically resolved soil biogeochemistry, explicit representation of ammonium and nitrate pools, and associated nitrification and denitrification fluxes (Koven et al., 2013). The major improvements in ELM v1 (Figure 1) compared to ELM v0, include (1) the implementation of a prognostic P cycle and CNP interactions, (2) the introduction of a

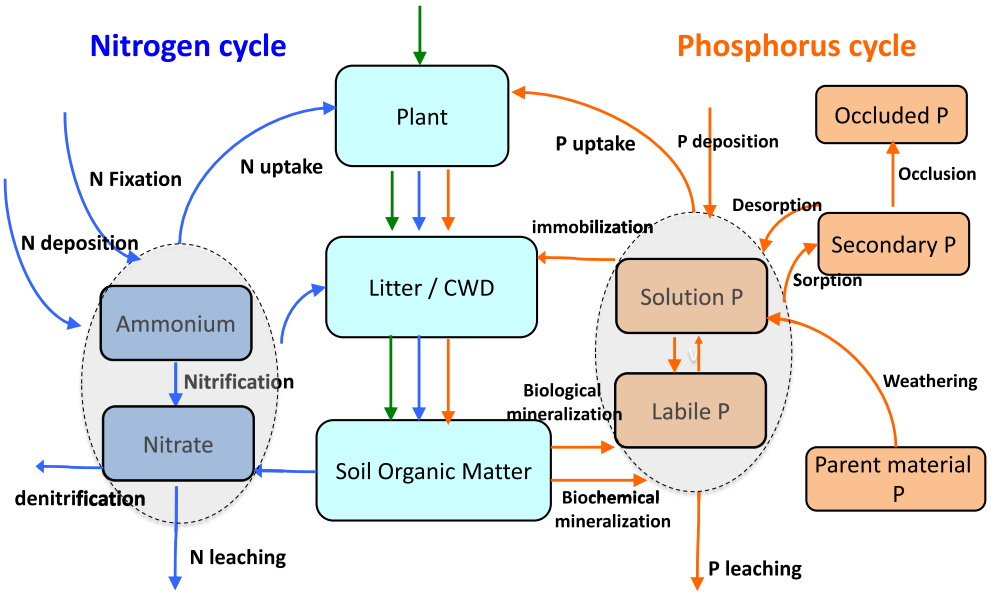

Figure 1. The model diagram of Energy Exascale Earth System Model land model. CWD, coarse woody debris; N, nitrogen; P, phosphorus.

soil-order-based mortality for tropical forests, and (3) the introduction of C, N, and P nonstructural vegetation storage pools.

We implemented a fully prognostic P cycle and CNP interactions into ELM v1. The major P pools and fluxes are based on our previous modeling study that implemented a P cycle into community land model 4 (Yang et al., 2014). There are five inorganic P pools, namely solution P, labile P, secondary mineral P, parent material P, and occluded P. Solution P represents the most readily available P. This pool can be directly taken up by plants and microbes and is rapidly replenished from the labile P pool when depleted. Labile P can become adsorbed onto secondary minerals and become secondary mineral P. Secondary mineral P can reenter labile P when desorption happens but at a much lower rate. Secondary mineral P is also gradually occluded to become occluded P. It is assumed that plants and microbes cannot access occluded P due to physical and chemical protections. The P inputs into ecosystems include atmospheric deposition and weathering, and the sole output flux is P leaching. Atmospheric P deposition is prescribed based on (Mahowald et al., 2005). P weathering flux is a function of weathering rate and parent material P. Plants and microbes can only take up P from solution P. Total flux of P for allocation to new growth is the sum of plant P uptake from soils and P flux due to resorption. Resorption flux of P is assumed to occur only during leaf turnover at a fixed fraction. P mineralization is represented in the model by biological mineralization associated with soil organic matter decomposition and biochemical mineralization through phosphatase activity. Biochemical mineralization of P is a function of the extent of P limitation, the extent of N limitation, and the size of soil organic P pool. P limitation on plant growth and soil decomposition are resolved based on a supply-demand approach, with supply controlled by the size of soil solution P and demand being the sum of plant and microbial demand. With both N and P limitations represented in the model, we employ the Liebig law to resolve the N versus P limitation, for example, the most limiting nutrient will determine the overall nutrient limitation. Detailed equations on the P cycle can be found in Yang et al. (2014). Here, we extend the original P cycle model into the vertically resolved structure in ELM v1, capturing the dynamics of inorganic P pools, the conversion between organic P and inorganic P in each soil layer, as well as the vertical transport of P pools between the layers.

The second major change we made in ELM v1 is the introduction of a simple approach to capture the soil physical structural controls on tree mortality, based on soil order. Galbraith et al. (2013) showed that edaphic factors exerted a strong influence on tree mortality in tropical forests, suggesting that tree mortality is lowest in highly weathered oxisols and highest in young soils. Quesada et al. (2009) found that mortality rate was significantly influenced by soil physical properties (topography, soil depth, and structure), which is

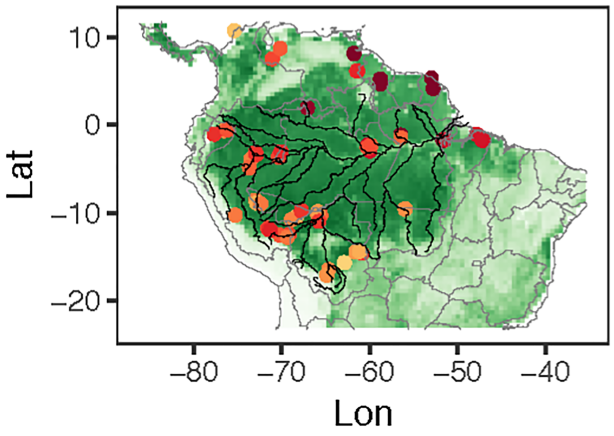

Figure 2. Map showing the study region and the locations of forest plots. The red dots represent the average of the measured aboveground biomass from the forest plots averaged to 0.5-degree grid cell. Darker color indicates higher aboveground biomass. Lat, latitude; Lon, longitude.

related to pedogenic development status. Poor soil physical properties such as shallow soil depths in young soils favor high mortality rates, while better soil physical properties in very old soils support low mortality rates (Quesada et al., 2012). We implement the relationship between soil order and tree mortality in tropical forests established in Galbraith et al. (2013) into ELM v1.

The third important change in ELM v1 is the implementation of the non-structural C, N, and P storage pools. Nutrients acquired by plant are first allocated to nonstructural nutrient storage pools. The availability of nutrients from the non-structural pools, compared with nutrient demand, determines the extent of nutrient limitation. Excess C due to nutrient limitation is allocated to a nonstructural C storage pool instead of instantaneous downregulation on GPP (Metcalfe et al., 2017). This excess C is respired to the atmosphere as an additional autotrophic respiration flux with a 3-year turnover time at 25 °C, which is modified by the same temperature function as for maintenance respiration. Allocation to structural plant pools is then calculated using available C and available nonstructural nutrients.

2.2. Model Configuration and Simulations

We performed two categories of simulations. The first category is a series of site level simulations at the grid cells where observational data are available (Figure 2). We ran the model with and without P limitation (carbon-nitrogen (CN) and CNP, see below for details) to evaluate the model performance at these sites. We also ran the model with constant mortality rates and with soil order based mortality rates to evaluate model simulated AGB at these sites. The second category is a series of regional simulations as summarized in Table 1. The region of study is shown in Figure 2. The simulations were performed at 0.5° × 0.5° spatial resolution. The model was first spun up for 1850 conditions, followed by historical transient simulations (1850–2010) with historical atmospheric (CO_2), N deposition (Lamarque et al., 2005), land use change (Hurtt, 2018), and Global Soil Wetness Project 3 (GSWP3) climate forcing (Dirmeyer et al., 2006). To investigate the role of P in affecting the responses of C fluxes to these forcing factors, two configurations of the model were used in this study: the CN only implementation of the model (denoted CN, which was executed with the same model code but assuming P saturation, for example, no P limitation on vegetation growth or decomposition) and the CNP version. We ran a suite of simulations to examine the individual and combined effects of changes in CO_2, climate, land use, and N deposition (Table 1). To investigate how the P cycle might affect

Table 1
Summary of Model Experiments Performed in the Amazon Region

Experiment	P coupling	CO2 forcing	LULCC	Climate forcing	N deposition
Hist_CN_CO_2	off	transient	1850	steady state[a]	1850
Hist_CNP_CO_2	on	transient	1850	steady state[a]	1850
Hist_CN_LUC	off	1850	transient	steady state[a]	1850
Hist_CNP_LUC	on	1850	transient	steady state[a]	1850
Hist_CN_climate	off	1850	1850	transient[b]	1850
Hist_CNP_climate	on	1850	1850	transient[b]	1850
Hist_CN_NDep	off	1850	1850	steady state[a]	transient
Hist_CNP_Ndep	on	1850	1850	steady state[a]	transient
Hist_CN_all	off	transient	transient	transient[b]	transient
Hist_CNP_all	on	transient	transient	transient[b]	transient
RCP45_CN_CO_2	off	RCP45 CO_2	same as 2010	cycling of GSWP3 (1991–2010)	same as 2010
RCP45_CNP_CO_2	on	RCP45 CO_2	same as 2010	cycling of GSWP3 (1991–2010)	same as 2010
RCP85_CN_CO_2	off	RCP85 CO_2	same as 2010	cycling of GSWP3 (1991–2010)	same as 2010
RCP85_CNP_CO_2	on	RCP85 CO_2	same as 2010	cycling of GSWP3 (1991–2010)	same as 2010

Abbreviations: GWSP, Global Soil Wetness Project; LULCC, land use and land cover change; N, nitrogen; P, phosphorus; RCP, Representative Concentration Pathway.
[a]Cycling of 20-year time series of GSWP3 reanalysis product (1901–1920). [b]Historical time series of GSWP3 reanalysis product (1901–2009).

the CO_2 fertilization effect in the future, we performed two sets of future simulations in which we used the atmospheric CO_2 concentrations from Representative Concentration Pathway (RCP) 8.5 and RCP 4.5(http://www.pik-potsdam.de/~mmalte/rcps/). For these future simulations, we first ran the model using historical atmospheric CO_2 and climate forcing until 2009. Starting from 2010, we ran model simulations for 90 more years with (1) prescribed atmospheric CO_2 concentrations from RCP 8.5 and RCP 4.5 (2) repetitively cycling the Global Soil Wetness Project 3 climate forcing data between 1991-2010 (3) keeping land cover and N deposition constant at 2010 values.

2.3. Field Observation Data

We used field observational data from permanent plots located throughout Amazonia, which were compiled and analyzed by Johnson et al. (2016), for model evaluation. Most of the plots are part of the RAINFOR, with additional data from TEAM networks (http://www.teamnetwork.org/) included. The AGB and aboveground woody productivity (W_P) data from 167 plots were included. These plots are all in undisturbed, old-growth forests with a mean plot size of 1.09 ha. The monitoring period is between 1995 and 2009; 76% of plot data are from 2000 to 2008. All trees with a diameter at breast height >10 cm were included in the analysis. The AGB values are based on the data from Mitchard et al. (2014). W_P was calculated based on repeated census of tree diameters within each plot with bias due to the census interval removed. Details about the observational data can be found in Johnson et al. (2016). To facilitate the comparison with model simulations, we aggregated the forest plot data into 0.5-degree grid cells. In total, there are 67 grid cells that have between one and nine plots in each grid cell (Figure 2).

3. Results

3.1. Model Evaluation Using Field Observations of AGB and W_P

We compared simulated wood productivity with field observed W_P from forest plots for model configurations with and without P limitation. Field observations showed that W_P tends to decrease from west to east (Figure 3a). The simulated W_P without P limitation shows little variation across the basin, while the simulation with P limitation is able to reproduce the decreasing trend from west to east, with a more consistent spatial variation compared to observations (Figure 3b and c). Mean simulated W_P across all plots from CN simulations is 3.75 $Mg{\cdot}ha^{-1}{\cdot}year^{-1}$. Mean simulated W_P across all the plots from CNP simulations is 3.11 $Mg{\cdot}ha^{-1}{\cdot}year^{-1}$, close to the mean W_P of 2.95 $Mg{\cdot}ha^{-1}{\cdot}yr^{-1}$ from forest plot measurements.

We also compared model simulated AGB with the field observed AGB. Field observations show a generally increasing pattern from west to east (Figure 4a). With the default assumption of constant mortality rate, model simulated AGB showed a decreasing trend from west to east, opposite to the pattern from field observations (Figure 4c). In contrast, the simulation with mortality rate based on soil order showed the consistent spatial pattern of above ground biomass with the observations (Figure 4b). Mean simulated AGB of (174 ± 55 $Mg{\cdot}ha^{-1}$), however, is overestimated compared with the observed values (143 ± 53 $Mg{\cdot}ha^{-1}$).

Model simulations at these mature forest sites suggest that these mature tropical forests have acted as a sustained C sink, but the magnitude of the sink has been decreasing (0.54-Mg C $ha^{-1}{\cdot}year^{-1}$ in 1980s, 0.5-Mg C $ha^{-1}{\cdot}year^{-1}$ in 1990s, and 0.45-Mg C $ha^{-1}{\cdot}year^{-1}$ in 2000s), which is consistent with field observations (Brienen et al., 2015). Phillips and Brienen (2017) showed that net gain in C in aboveground forest biomass is 0.37-Mg C $ha^{-1}{\cdot}year^{-1}$ in the 1980s and 1990s and 0.24-Mg C $ha^{-1}{\cdot}year^{-1}$ in the 2000's.

3.2. Historical Simulation Results

Model simulations show that increasing CO_2 leads to a sustained C sink (the increase in total ecosystem C) in the Amazon region due to the CO_2 fertilization effect, which results in accumulation of C in both vegetation and soils (Figure 5a, c, and e and Figure 7a and b). The accumulation of C induced by increasing CO_2 is smaller in CNP simulation because available P in soils is not sufficient to satisfy the increasing P demand driven by increased productivity under elevated CO_2. The difference between the CN and CNP simulations becomes progressively greater between 1900 and 2010, suggesting P is becoming increasingly limiting (Figure 5a, c, and e). Across the region, the CO_2 fertilization effect is most pronounced in the forested area, where productivity is higher (Figure 7a and b). The effect of P limitation on CO_2-induced C sink is spatially

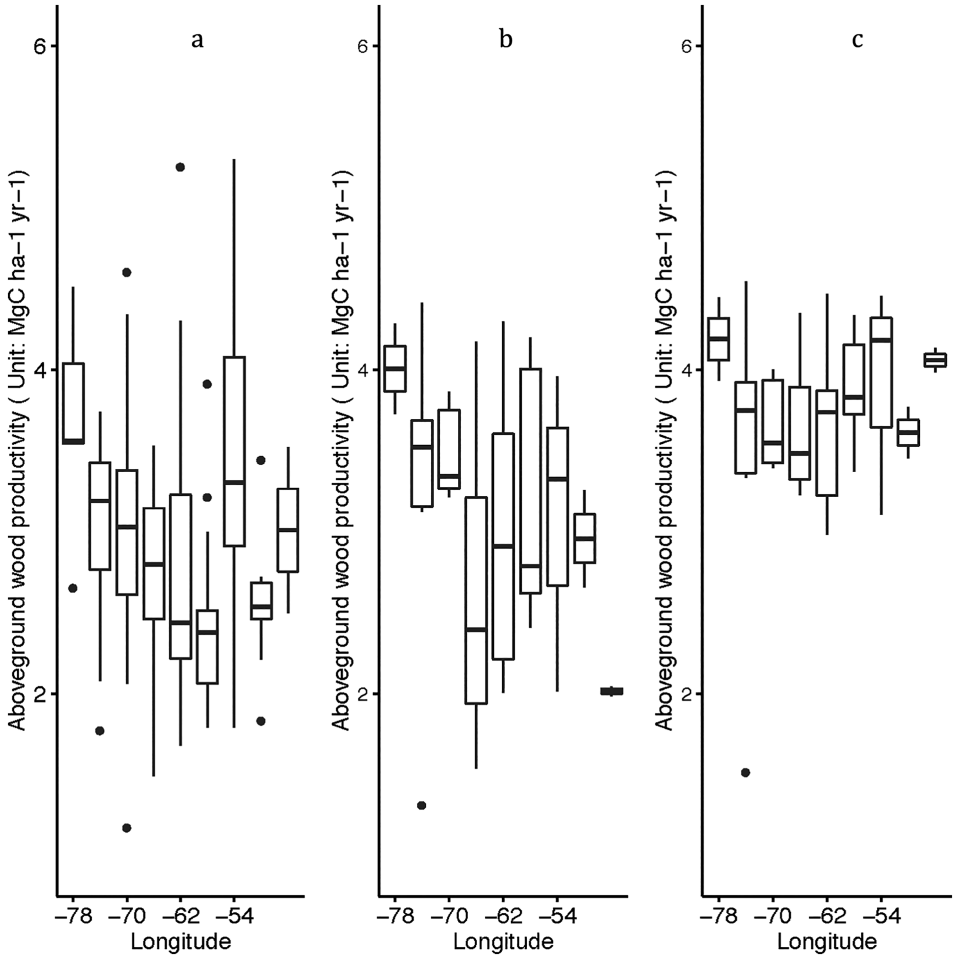

Figure 3. Comparison of model simulated aboveground wood productivity with field observations. (a) field observations (b) carbon-nitrogen-phosphorus (CNP) (c) carbon-nitrogen (CN).

heterogeneous, and the effect is most significant in the central and eastern parts of the Amazon basin (Figure 7c).

Model simulations show that LULCC is a significant C source in the Amazon region for both CN and CNP simulations, which results in continual loss of C during 1900 and 2010, especially for vegetation C (Figure 5b, d, and f). The loss of C is much greater in CN simulation because of increased C stock when P limitation is not considered. In the CNP simulation, P limitation leads to reduced productivity, reduced vegetation C stock, and therefore the less C loss with LULCC. C emissions associated with LULCC are highest along the southeastern edge of the Amazon basin where deforestation is concentrated (Figure 7d and e). The influence of P availability on the LULCC C emission is also more pronounced in these areas (Figure 7f).

Our simulations show that although climate condition leads to large year-to-year variability in C fluxes, over the long-term effects of climate on C stocks are very small (Figure not shown). The effects of N deposition on the C stocks is also minimal compared with the effects of CO_2 and LULCC (Figure not shown).

The combined effects of CO_2, climate, land-use change, and N deposition generally lead to an increase of C from 1900 to 2010 across the Amazon region in both CNP simulation and CN simulations (Figure 6). Most of the C accumulation occurs in vegetation biomass (Figure 6a and b). The sink strength, however, is much smaller in CNP simulations as the CO_2 fertilization effect is constrained by soil P availability. The effect of P on C fluxes is spatially heterogeneous across the study region. Consideration of P leads to smaller C sink in most areas in the Amazon basin, especially the central and eastern part of the basin (Figure 7i). In these regions, tropical forests become C neutral in CNP simulations, while acting as small sinks in the CN

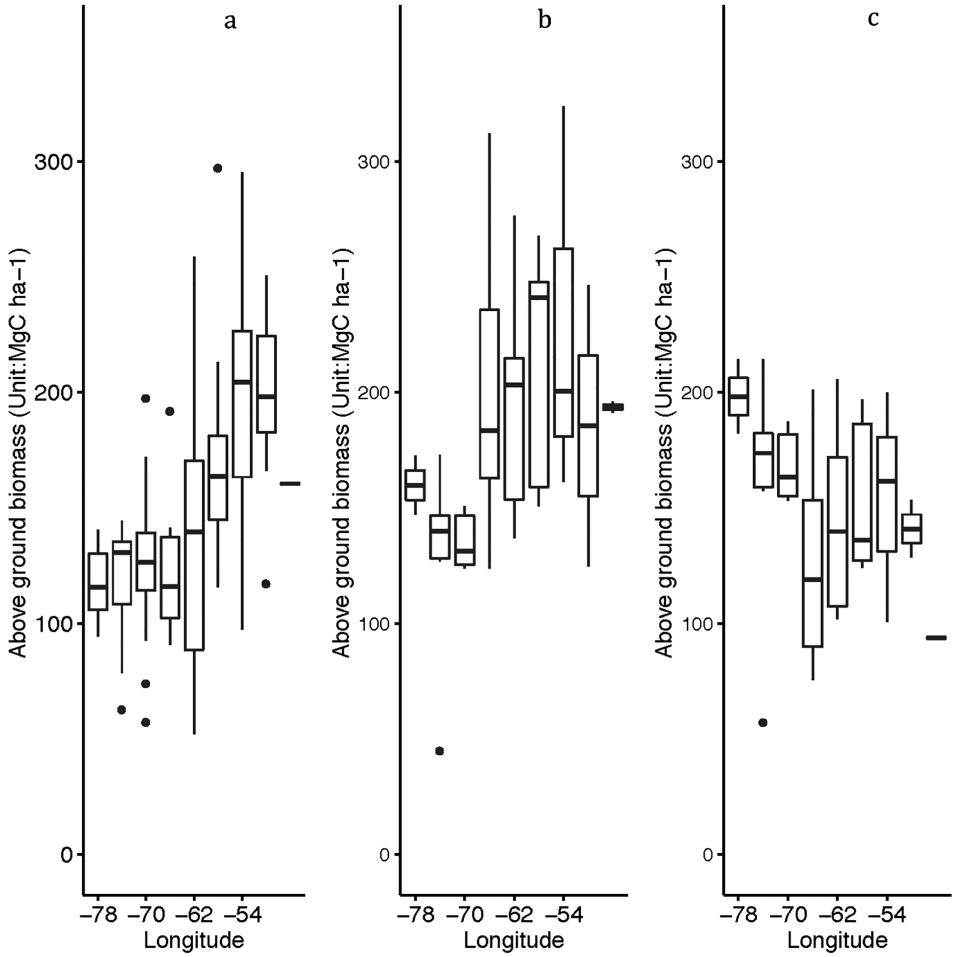

Figure 4. Comparison of model simulated aboveground biomass with field observations. (a) Field observations, (b) soil order based mortality, and (c) constant mortality.

simulations (Figure 7g and h). Near the southeastern edge of the basin where deforestation is concentrated, consideration of P leads to a smaller source of C due to the reduced C stock associated with diminished productivity caused by P limitation (Figure 7i).

3.3. Results With RCP4.5 and RCP8.5 CO_2 Concentrations

CO_2 fertilization leads to a sustained C sink under RCP8.5 and RCP4.5, but P limitation on productivity can significantly reduce the C sink (Figure 8). By the end of the 21st century, Amazon ecosystems without P limitation take up about 85-Pg C under the "unmitigated business-as-usual" CO_2 emissions scenario (RCP8.5) and about 56-Pg C under the "mitigated business-as-usual" CO_2 emissions scenario (RCP4.5). However, as CO_2 concentration increases, the increased productivity leads to increasing demand for nutrients, especially P in Amazon region. The supply of P, however, cannot keep up with the increasing P demand, which leads to the reduction of C sink. Model simulations suggest that, by 2100, the Amazon ecosystem takes up about 52-Pg C under RCP8.5 and 28-Pg C under RCP4.5, when P limitation is considered.

4. Discussion

4.1. Spatial Patterns of Productivity and Biomass

Results of this study suggest that soil edaphic factors must be considered in order to capture the observed spatial pattern of productivity and biomass in the Amazon region. Consideration of soil P availability improved model simulated productivity, enabling the model to capture the productivity gradient from

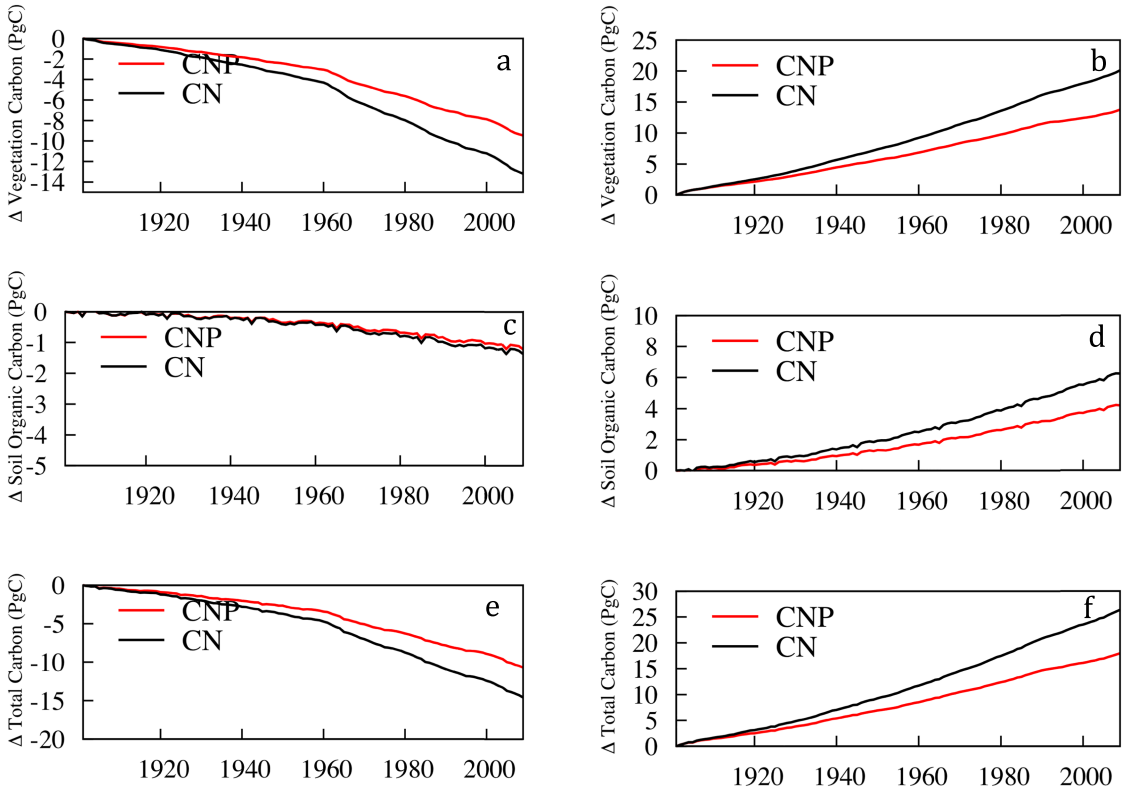

Figure 5. Simulated change in land carbon storage in response to historical increase in CO_2 (a, c, and e) and land use and land cover change (1900–2009; b, d, and f): vegetation carbon(a and b), soil carbon(c and d), and total ecosystem carbon(e and f) based on CNP and CN. Unit: Pg C. CN, carbon-nitrogen; CNP, carbon-nitrogen-phosphorus.

west to east across the Amazon basin. Consideration of the effect of soil physical state and soil development stages on tree mortality allows us to capture the spatial pattern of above ground biomass across the basin. Model simulated C accumulation in undisturbed forests agrees with forest inventory observations (Brienen et al., 2015; Phillips & Brienen, 2017). None of the four dynamic global vegetation models in Castanho et al. (2016) were able to reproduce the observed west-east gradient of productivity and biomass across the basin, mostly likely due to the lack of consideration of P cycle impacts on the C cycle and the lack of treatment of soil properties on vegetation C turnover. The only model that was able to capture the spatial pattern of biomass and productivity was IBIS-HP (Integrated Biosphere Simulator - Heterogeneous Parameterization), which implemented spatial varying plant traits parameterization based on observed soil P availability and tree mortality rate (Castanho et al., 2013). Delbart et al. (2010) explored the idea of relating mortality to productivity, which was developed based on forest plot data mostly in western Amazon and a few east-central plots (Malhi, 2012); this approach resulted in improved spatial variation of biomass. (Johnson et al., 2016), however, found that with a broad range of sites, there is no correlation between W_P and mortality rate. As an alternative approach, mortality based on soil order is simple, observation-based, and results in the improved simulated spatial gradient of AGB.

The simulated total above ground biomass is 114-Pg C for the study region, very close to the 108-Pg C estimated by (Baccini et al., 2012) for tropical America which used multisensor satellite data for the estimate of AGB C for tropical ecosystems with unprecedented accuracy and spatial resolution. The improved estimate of vegetation biomass distribution not only allows us to have an accurate understanding of C stocks but also provides a more accurate basis for estimating C emissions due to deforestation.

4.2. Historical C Sources and Sinks

This study investigated the importance of increasing CO_2 and LULCC as main drivers of the Amazon C balance during historical time period and how the consideration of P cycling and P limitation affects the C fluxes associated with these drivers. Our factorial analysis suggests that the sustained C sink in these

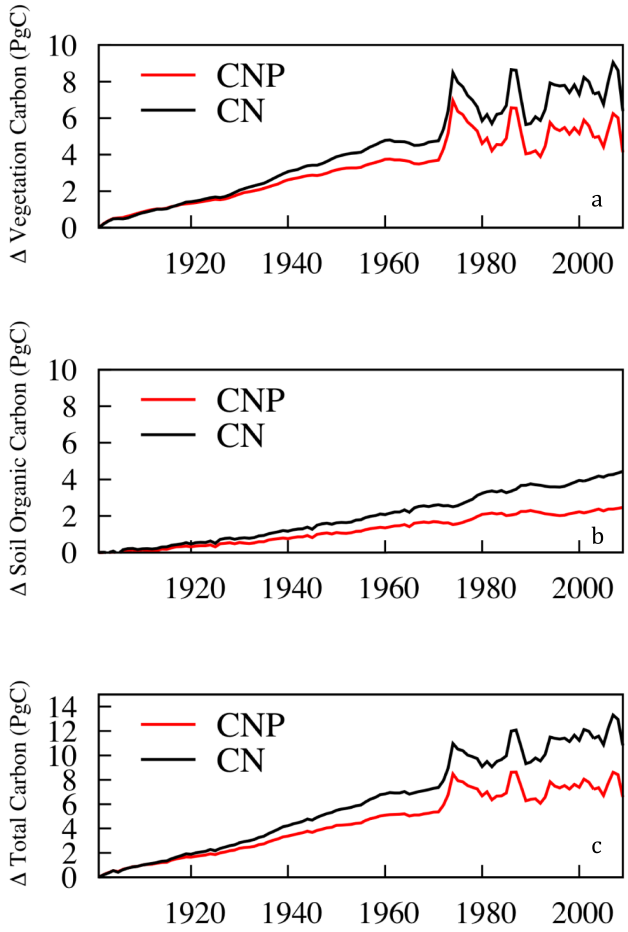

Figure 6. Simulated change in land carbon storage in response to historical increase in CO_2, land use and land cover change, climate, and N deposition (1900–2009): vegetation carbon(a), soil carbon(b), and total ecosystem carbon(c) based on CNP and CN. Unit: Pg C. CN, carbon-nitrogen; CNP, carbon-nitrogen-phosphorus; N, nitrogen.

undisturbed forests is mainly caused by the CO_2 fertilization effect. The accumulated CO_2 fertilization effect between 1850 and 2010 is 58.79-Pg C for CN simulations and 40.39-Pg C for CNP simulations, suggesting a 31% reduction of CO2 fertilization effect because of P limitation. This is slightly higher than the 25% reduction from Yang et al. (2016). Smith et al. (2016) compared the estimated fertilization effect derived from satellite-based NPP with the ESM-derived estimate and found that satellite-derived estimate is less than half of the estimate based on Earth System Models (ESMs). They further suggested that the large divergence between these two is potentially due to a lack of representation of nutrient constraints, which is consistent with the findings of this study. LULCC has been a substantial source of C to the atmosphere, with the magnitude of emissions comparable to the CO_2 fertilization effect. In the CN simulation, land-use changes led to 37.85 Pg of C released to the atmosphere between 1850–2000. CNP simulations estimated the C loss of 26.63-Pg C during 1850–2000, with the difference mainly due to less biomass when there is diminished productivity associated with P limitation. The results indicate that better estimates of C stocks are crucial to improving the estimates of C fluxes associated with human disturbances such as land cover and land use, and improving the representation of nutrient dynamics and nutrient constraint on productivity is essential to achieve this.

Although in the long-term sources and sinks of C are dominated by the CO_2 fertilization effect and deforestation, model simulations show that there is a significant interannual variability in C fluxes in the Amazon region, mainly driven by climate variability. The Amazon region acts as a C sink in wet years while becoming a source of C during drought. For example, model results suggest that the Amazon basin was a C sink during 2000–2010. In 2005 and 2010 when the Amazon experienced significant drought associated with El Nino, it became a big source of C, releasing 0.13-Pg C in 2005 and 0.37-Pg C in 2010. These results are consistent with the findings from field plots and satellite studies showing that intact tropical forests become a source of C in unusually hot and dry years (Brienen et al., 2015; Liu et al., 2017; Phillips et al., 2009).

4.3. Future C Sink and P Limitation

Our simulations suggest that including P limitation is critical for projecting future C uptake in tropical ecosystems. Without considering P limitation, we would overestimate the ability of tropical forests to assimilate atmospheric CO_2. Our findings are consistent with previous studies that evaluated how simulated CO_2 fertilization effects among Coupled Model Intercomparison Project phase 5 (CMIP5) models could be constrained by N and P availability (Sun et al., 2017; Wieder et al., 2015), but here, we provide a quantitative estimate of the extent of P limitation through explicit modeling of P cycle dynamics and CNP interactions. Our findings are also consistent with other theoretical studies that suggest the potential for P limitation to ultimately constrain terrestrial C storage in tropical ecosystems (Peñuelas et al., 2013; Vitousek et al., 2010), and supported by indirect evidence from a meta-analysis of C-nutrient-climate relationships in lowland tropical forests (Cleveland et al., 2011). It is worth mentioning that since few nutrient manipulation experiments have been conducted in the Amazon, the direct evidence for P limitation in Amazon lowland tropical forests is limited. Experimental studies on lowland tropical forests elsewhere in the neotropics provide mixed evidence. Fertilization experiments in Panama tropical forests found an increase in litterfall with P addition but also show strong response to N and potassium addition (Wright et al., 2011). It has also been found that P limitation is pervasive at the species level but not at the community level across a steep natural P gradient in Panama tropical forests (Alvarez-Clare et al., 2013; Condit et al., 2013; Turner et al., 2018). Wright et al. (2018) found that plant responses to P addition are not stronger than to N addition, but they

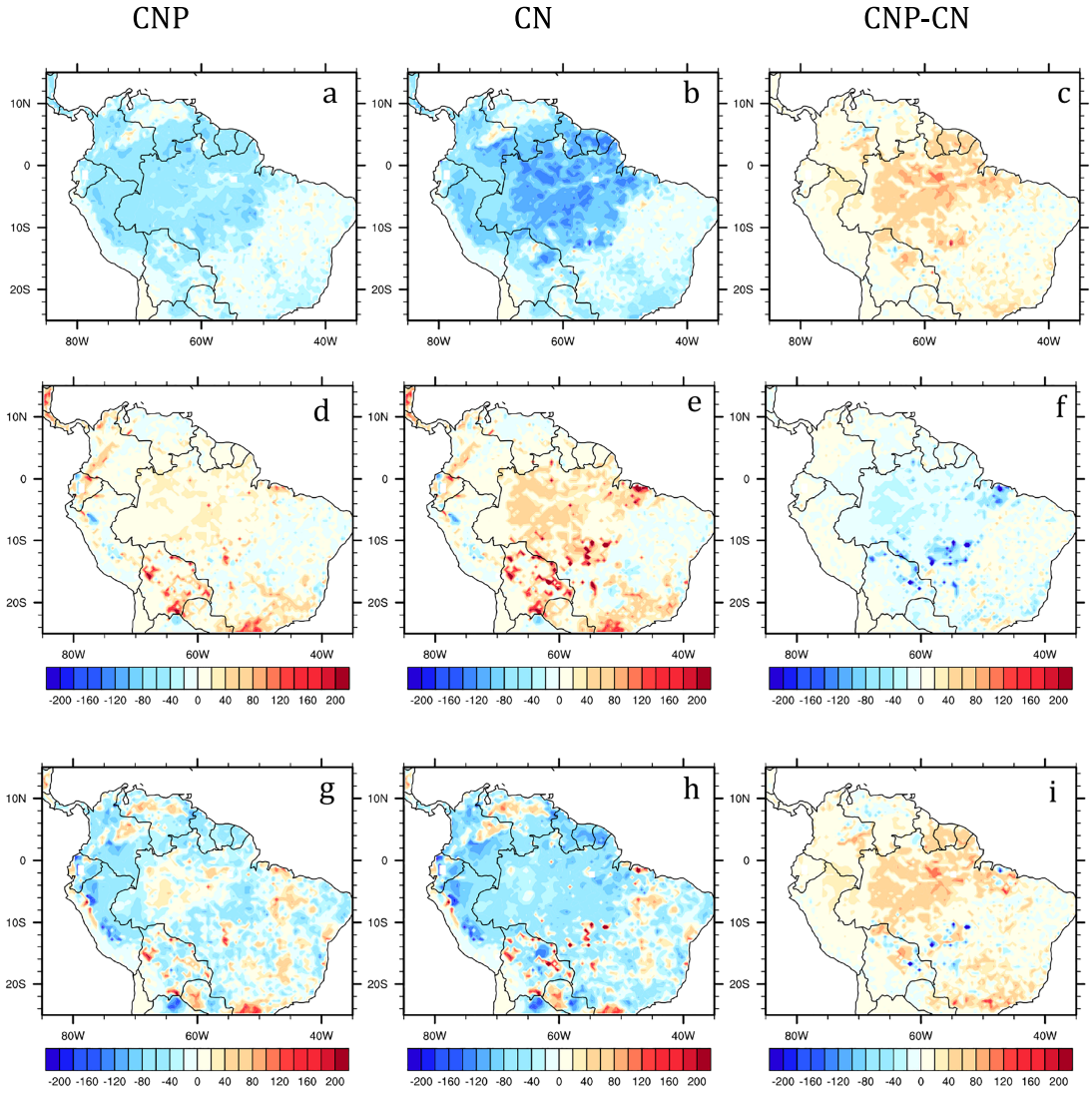

Figure 7. Map of carbon fluxes associated with increasing CO2 (a–c), land cover and land-use change (d–f), and all environmental factors (g–i) between 2000–2009. The first column (a, d, and g) is for CNP configurations, the second column (b, e, and h) is for CN configurations, and the third column is for CNP minus CN. Hot colors indicate release of carbon from ecosystems and cold colors indicate carbon uptake by ecosystems. Unit: gC m^{-2} $year^{-1}$. CN, carbon-nitrogen; CNP, carbon-nitrogen-phosphorus.

also pointed out their findings are not conclusive because of small numbers of experiments, insufficient statistical power, and especially the short duration of the experiments. We advocate more long-term nutrient manipulation experiments in the Amazon tropical forests to help us better understand the importance of P limitation in lowland tropical forests.

Although ELM-v1 considers all major P cycle processes, including mechanisms that can relieve P limitation with increasing P demand under elevated CO_2 (e.g., phosphatase activity), there are still large uncertainties in the availability and dynamics of soil P. For example, it has been suggested occluded P can become available to plants through mycorrhizal associations (Richter et al., 2006). The active role of plant in P acquisition through root exudation, changing allocation, and flexible stoichiometry are also not included in these simulations, which could help alleviate P limitation under elevated CO_2 (Buendía et al., 2014). Further studies are needed to help understand and quantify the relative roles of different P acquisition strategies. We are also not considering the accelerated mineralization of soil P from warming in these RCP simulations, which may help relieve P limitation to some extent under elevated CO_2 (Wood et al., 2012). However, the effects may be limited as mineralized P would be rapidly sorbed

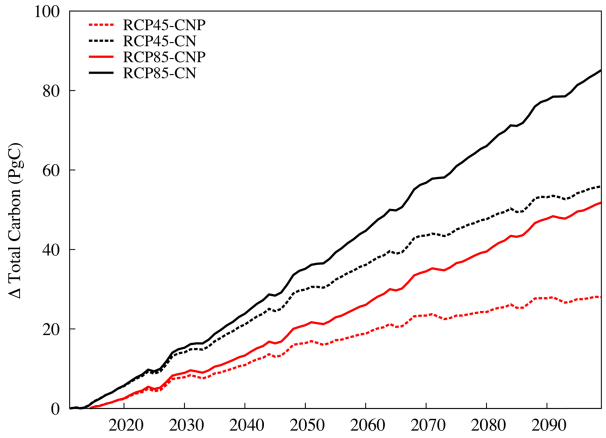

Figure 8. Simulated change in land carbon storage in response to changes in CO_2 (2010–2100) under RCP8.5 and RCP4.5 CO2 emission scenarios. Unit: Pg C. CN, carbon-nitrogen; CNP, carbon-nitrogen-phosphorus; RCP, Representative Concentration Pathway.

onto clay-rich minerals in tropical soils, and large effects may be unlikely over the long-term as labile soil organic pools become rapidly depleted (Wieder et al., 2015).

5. Conclusions

In this study, we show that the implementation of P cycle and P limitation in the ELM v1 improves the simulated spatial pattern of wood productivity. The P-enabled ELM-v1 is able to capture the west-to-east gradient of productivity, consistent with field observations. We also show that by improving the representation of mortality processes, ELMv1 is able to reproduce the observed spatial pattern of above ground biomass. Our model simulations show that the consideration of P availability lead to a smaller C sink associated with CO_2 fertilization, and lower C emissions due to LULCC. Simulations under future CO_2 scenarios suggest that P limitation is critical for projecting future C uptake in tropical ecosystems. Our results have important implications for projections of future C balance in the Amazon region. Recent climate models suggested that the Amazon C sink is resilient (Cox et al., 2013; Huntingford et al., 2013; Rammig et al., 2010) mainly due to the CO_2 fertilization effect. However, these studies have not considered the constraint of P availability on CO_2 fertilization. If P limitation is considered, the projected C sink would become much smaller. Furthermore, climate change will likely lead to increasing temperature and drought condition, which will further increase soil and plant respiration rate and lead to loss of C from the ecosystems. Combined with the possible decrease of the area of intact tropical forests that act currently as C sink, the Amazon region may become a source of C in the future.

We have identified some data needs that will help improve model representation, enable model testing, and improve predictions. For example, it would be helpful to expand the plot network for field data to provide better benchmarks for model testing. The recent development of a large database of NPP and biomass across tropical forests sites in Central and South America, Asia and Australasia will be useful for further model evaluation and development (Taylor et al., 2019). We need field experiments that manipulate environmental factors such as CO_2, precipitation, and temperature to help us improve our understanding of how tropical forests would respond to future CO_2 and climate (Norby et al., 2016; Reed et al., 2015). In particular, we need to better understand how P cycle might respond to changes in environmental conditions and how that might affect tropical ecosystem responses. As we learned from this study, P cycling and limitation have great impacts on the sources and sinks of C in the Amazon region.

Acknowledgments
This research was supported as part of the E3SM project, funded by the U.S. Department of Energy, Office of Science, Office of Biological and Environmental Research. R. J. Norby was supported as part of the Next Generation Ecosystem Experiments-Tropics, funded by the U.S. Department of Energy, Office of Science, Office of Biological and Environmental Research. F. M. Hoffman and M. Xu were supported by the Reducing Uncertainties in Biogeochemical Interactions through Synthesis and Computation Scientific Focus Area, which is sponsored by the Regional and Global Model Analysis Program in the Climate and Environmental Sciences Division of the Office of Biological and Environmental Research in the U.S. Department of Energy Office of Science. The source code, input data, and comp set for the simulations are available at https://github.com/E3SM-Project/E3SM. The model data used in this study can be downloaded at the website https://portal.nersc.gov/project/acme/xyk/datashare_YangEtAl.tar. This research used resources of the Compute and Data Environment for Science at the Oak Ridge National Laboratory, which is supported by the Office of Science of the U.S. Department of Energy under Contract DE-AC05-00OR22725.

References

Alvarez-Clare, S., Mack, M. C., & Brooks, M. (2013). A direct test of nitrogen and phosphorus limitation to net primary productivity in a lowland tropical wet forest. *Ecology*, *94*(7), 1540–1551. https://doi.org/10.1890/12-2128.1

Aragão, L., Malhi, Y., Metcalfe, D., Silva-Espejo, J., Jimenez, E., Navarrete, D., et al. (2009). Above-and below-ground net primary productivity across ten Amazonian forests on contrasting soils. *Biogeosciences*, *6*(12), 2759–2778. https://doi.org/10.5194/bg-6-2759-2009

Avitabile, V., Herold, M., Heuvelink, G. B., Lewis, S. L., Phillips, O. L., Asner, G. P., et al. (2016). An integrated pan-tropical biomass map using multiple reference datasets. *Global Change Biology*, *22*(4), 1406–1420. https://doi.org/10.1111/gcb.13139

Baccini, A., Goetz, S., Walker, W., Laporte, N., Sun, M., Sulla-Menashe, D., et al. (2012). Estimated carbon dioxide emissions from tropical deforestation improved by carbon-density maps. *Nature Climate Change*, *2*(3), 182–185. https://doi.org/10.1038/nclimate1354

Brienen, R. J., Phillips, O. L., Feldpausch, T. R., Gloor, E., Baker, T. R., Lloyd, J., et al. (2015). Long-term decline of the Amazon carbon sink. *Nature*, *519*(7543), 344–348. https://doi.org/10.1038/nature14283

Buendía, C., Arens, S., Hickler, T., Higgins, S., Porada, P., & Kleidon, A. (2014). On the potential vegetation feedbacks that enhance phosphorus availability–insights from a process-based model linking geological and ecological timescales. *Biogeosciences*, *11*(13), 3661–3683. https://doi.org/10.5194/bg-11-3661-2014

Castanho, A., Coe, M., Costa, M., Malhi, Y., Galbraith, D., & Quesada, C. (2013). Improving simulated Amazon forest biomass and productivity by including spatial variation in biophysical parameters. *Biogeosciences*, *10*(4), 2255–2272. https://doi.org/10.5194/bg-10-2255-2013

Castanho, A., Galbraith, D., Zhang, K., Coe, M. T., Costa, M. H., & Moorcroft, P. (2016). Changing Amazon biomass and the role of atmospheric CO2 concentration, climate, and land use. *Global Biogeochemical Cycles*, *30*, 18–39. https://doi.org/10.1002/2015GB005135

Clark, D. A., Clark, D. B., & Oberbauer, S. F. (2013). Field-quantified responses of tropical rainforest aboveground productivity to increasing CO2 and climatic stress, 1997–2009. *Journal of Geophysical Research: Biogeosciences*, *118*, 783–794. https://doi.org/10.1002/jgrg.20067

Cleveland, C. C., Townsend, A. R., Taylor, P., Alvarez-Clare, S., Bustamante, M., Chuyong, G., et al. (2011). Relationships among net primary productivity, nutrients and climate in tropical rain forest: A pan-tropical analysis. *Ecology Letters*, *14*(9), 939–947. https://doi.org/10.1111/j.1461-0248.2011.01658.x

Condit, R., Engelbrecht, B. M., Pino, D., Pérez, R., & Turner, B. L. (2013). Species distributions in response to individual soil nutrients and seasonal drought across a community of tropical trees. *Proceedings of the National Academy of Sciences*, *110*(13), 5064–5068. https://doi.org/10.1073/pnas.1218042110

Cox, P. M., Pearson, D., Booth, B. B., Friedlingstein, P., Huntingford, C., Jones, C. D., & Luke, C. M. (2013). Sensitivity of tropical carbon to climate change constrained by carbon dioxide variability. *Nature*, *494*(7437), 341–344. https://doi.org/10.1038/nature11882

Delbart, N., Ciais, P., Chave, J., Viovy, N., Malhi, Y., & Le Toan, T. (2010). Mortality as a key driver of the spatial distribution of above-ground biomass in Amazonian forest: Results from a dynamic vegetation model. *Biogeosciences*, *7*(10), 3027–3039. https://doi.org/10.5194/bg-7-3027-2010

Dirmeyer, P. A., Gao, X., Zhao, M., Guo, Z., Oki, T., & Hanasaki, N. (2006). GSWP-2: Multimodel analysis and implications for our perception of the land surface. *Bulletin of the American Meteorological Society*, *87*(10), 1381–1398. https://doi.org/10.1175/BAMS-87-10-1381

Galbraith, D., Levy, P. E., Sitch, S., Huntingford, C., Cox, P., Williams, M., & Meir, P. (2010). Multiple mechanisms of Amazonian forest biomass losses in three dynamic global vegetation models under climate change. *New Phytologist*, *187*(3), 647–665. https://doi.org/10.1111/j.1469-8137.2010.03350.x

Galbraith, D., Malhi, Y., Affum-Baffoe, K., Castanho, A. D., Doughty, C. E., Fisher, R. A., et al. (2013). Residence times of woody biomass in tropical forests. *Plant Ecology and Diversity*, *6*(1), 139–157. https://doi.org/10.1080/17550874.2013.770578

Goll, D., Brovkin, V., Parida, B., Reick, C., Kattge, J., Reich, P., et al. (2012). Nutrient limitation reduces land carbon uptake in simulations with a model of combined carbon, nitrogen and phosphorus cycling. *Biogeosciences*, *9*(9), 3547–3569. https://doi.org/10.5194/bg-9-3547-2012

Hedin, L. O. (2015). Biogeochemistry: Signs of saturation in the tropical carbon sink. *Nature*, *519*(7543), 295–296. https://doi.org/10.1038/519295a

Houghton, R. A., Skole, D., Nobre, C. A., Hackler, J., Lawrence, K., & Chomentowski, W. H. (2000). Annual fluxes of carbon from deforestation and regrowth in the Brazilian Amazon. *Nature*, *403*(6767), 301–304. https://doi.org/10.1038/35002062

Huntingford, C., Zelazowski, P., Galbraith, D., Mercado, L. M., Sitch, S., Fisher, R., et al. (2013). Simulated resilience of tropical rainforests to CO 2-induced climate change. *Nature Geoscience*, *6*(4), 268–273. https://doi.org/10.1038/ngeo1741

Hurtt, G. (2018). Enabling land-use in E3SM land model. Rep., University of Maryland.

Johnson, M. O., Galbraith, D., Gloor, M., De Deurwaerder, H., Guimberteau, M., Rammig, A., et al. (2016). Variation in stem mortality rates determines patterns of above-ground biomass in Amazonian forests: Implications for dynamic global vegetation models. *Global Change Biology*, *22*(12), 3996–4013. https://doi.org/10.1111/gcb.13315

Koven, C., Riley, W., Subin, Z., Tang, J., Torn, M., Collins, W., et al. (2013). The effect of vertically resolved soil biogeochemistry and alternate soil C and N models on C dynamics of CLM4. *Biogeosciences*, *10*(11), 7109–7131. https://doi.org/10.5194/bg-10-7109-2013

Lamarque, J. F., Kiehl, J., Brasseur, G., Butler, T., Cameron-Smith, P., Collins, W., et al. (2005). Assessing future nitrogen deposition and carbon cycle feedback using a multimodel approach: Analysis of nitrogen deposition. *Journal of Geophysical Research*, *110*, D19303. https://doi.org/10.1029/2005JD005825

Liu, J., Bowman, K. W., Schimel, D. S., Parazoo, N. C., Jiang, Z., Lee, M., et al. (2017). Contrasting carbon cycle responses of the tropical continents to the 2015–2016 El Niño. *Science*, *358*, eaam5690. https://doi.org/10.1126/science.aam5690

Mahowald, N. M., Baker, A. R., Bergametti, G., Brooks, N., Duce, R. A., Jickells, T. D., et al. (2005). Atmospheric global dust cycle and iron inputs to the ocean. *Global Biogeochem Cycles*, *19*(4), GB4025. https://doi.org/10.1029/2004GB002402

Malhi, Y. (2012). The productivity, metabolism and carbon cycle of tropical forest vegetation. *Journal of Ecology*, *100*(1), 65–75. https://doi.org/10.1111/j.1365-2745.2011.01916.x

Malhi, Y., Aragao, L. E. O., Metcalfe, D. B., Paiva, R., Quesada, C. A., Almeida, S., et al. (2009). Comprehensive assessment of carbon productivity, allocation and storage in three Amazonian forests. *Global Change Biology*, *15*(5), 1255–1274. https://doi.org/10.1111/j.1365-2486.2008.01780.x

Malhi, Y., Baker, T. R., Phillips, O. L., Almeida, S., Alvarez, E., Arroyo, L., et al. (2004). The above-ground coarse wood productivity of 104 neotropical forest plots. *Global Change Biology*, *10*(5), 563–591. https://doi.org/10.1111/j.1529-8817.2003.00778.x

Metcalfe, D. B., Ricciuto, D., Palmroth, S., Campbell, C., Hurry, V., Mao, J., et al. (2017). Informing climate models with rapid chamber measurements of forest carbon uptake. *Global Change Biology*, *23*(5), 2130–2139. https://doi.org/10.1111/gcb.13451

Mitchard, E. T. (2018). The tropical forest carbon cycle and climate change. *Nature*, *559*(7715), 527–534. https://doi.org/10.1038/s41586-018-0300-2

Mitchard, E. T., Feldpausch, T. R., Brienen, R. J., Lopez-Gonzalez, G., Monteagudo, A., Baker, T. R., et al. (2014). Markedly divergent estimates of Amazon forest carbon density from ground plots and satellites. *Global Ecology and Biogeography*, *23*(8), 935–946. https://doi.org/10.1111/geb.12168

Norby, R. J., De Kauwe, M. G., Domingues, T. F., Duursma, R. A., Ellsworth, D. S., Goll, D. S., et al. (2016). Model–data synthesis for the next generation of forest free-air CO2 enrichment (FACE) experiments. *New Phytologist*, *209*(1), 17–28. https://doi.org/10.1111/nph.13593

Oleson, K., Lawrence, D., Bonan, G., Drewniak, B., Huang, M., Koven, C., et al. (2013). Technical description of version 4.5 of the community land model (CLM) (NCAR/TN-503+STR). Boulder, CO: National Center for Atmospheric Research. https://doi.org/10.5065/D6RR1W7M

Pan, Y., Birdsey, R. A., Fang, J., Houghton, R., Kauppi, P. E., Kurz, W. A., et al. (2011). A large and persistent carbon sink in the world's forests. *Science*, *333*(6045), 988–993. https://doi.org/10.1126/science.1201609

Peñuelas, J., Poulter, B., Sardans, J., Ciais, P., van der Velde, M., Bopp, L., et al. (2013). Human-induced nitrogen–phosphorus imbalances alter natural and managed ecosystems across the globe. *Nature Communications*, *4*(1), 2934. https://doi.org/10.1038/ncomms3934

Phillips, O. L., Aragão, L. E. O. C., Lewis, S. L., Fisher, J. B., Lloyd, J., López-González, G., et al. (2009). Drought sensitivity of the Amazon rainforest. *Science*, *323*(5919), 1344–1347. https://doi.org/10.1126/science.1164033

Phillips, O. L., Brienen, R. J., & R. collaboration (2017). Carbon uptake by mature Amazon forests has mitigated Amazon nations' carbon emissions. *Carbon Balance and Management*, *12*(1), 1. https://doi.org/10.1186/s13021-016-0069-2

Quesada, C., Lloyd, J., Schwarz, M., Patino, S., Baker, T. R., Czimczik, C., et al. (2009). Chemical and physical properties of Amazon forest soils in relation to their genesis. *Biogeosciences Discussions*, *6*(2), 3923–3992. https://doi.org/10.5194/bgd-6-3923-2009

Quesada, C., Phillips, O., Schwarz, M., Czimczik, C., Baker, T., PatiÃ±o, S., et al. (2012). Basin-wide variations in Amazon forest structure and function are mediated by both soils and climate. *Biogeosciences*, *9*(6), 2203–2246. https://doi.org/10.5194/bg-9-2203-2012

Rammig, A., Jupp, T., Thonicke, K., Tietjen, B., Heinke, J., Ostberg, S., et al. (2010). Estimating the risk of Amazonian forest dieback. *New Phytologist*, *187*(3), 694–706. https://doi.org/10.1111/j.1469-8137.2010.03318.x

Reed, S. C., Yang, X., & Thornton, P. E. (2015). Incorporating phosphorus cycling into global modeling efforts: A worthwhile, tractable endeavor. *New Phytologist*, *208*(2), 324–329. https://doi.org/10.1111/nph.13521

Ricciuto, D., Sargsyan, K., & Thornton, P. (2018). The impact of parametric uncertainties on biogeochemistry in the E3SM land model. *Journal of Advances in Modeling Earth Systems*, *10*(2), 297–319. https://doi.org/10.1002/2017MS000962

Richter, D. D., Allen, H. L., Li, J., Markewitz, D., & Raikes, J. (2006). Bioavailability of slowly cycling soil phosphorus: Major restructuring of soil P fractions over four decades in an aggrading forest. *Oecologia*, *150*(2), 259–271. https://doi.org/10.1007/s00442-006-0510-4

Smith, W. K., Reed, S. C., Cleveland, C. C., Ballantyne, A. P., Anderegg, W. R., Wieder, W. R., et al. (2016). Large divergence of satellite and Earth system model estimates of global terrestrial CO 2 fertilization. *Nature Climate Change*, *6*(3), 306–310. https://doi.org/10.1038/nclimate2879

Sun, Y., Peng, S., Goll, D. S., Ciais, P., Guenet, B., Guimberteau, M., et al. (2017). Diagnosing phosphorus limitations in natural terrestrial ecosystems in carbon cycle models. *Earth's Future*, *5*(7), 730–749. https://doi.org/10.1002/2016EF000472

Taylor, P. G., Cleveland, C. C., Soper, F., Wieder, W. R., Dobrowski, S. Z., Doughty, C. E., & Townsend, A. R. (2019). Greater stem growth, woody allocation, and aboveground biomass in Paleotropical forests than in neotropical forests. *Ecology*, *100*(3), e02589. https://doi.org/10.1002/ecy.2589

Tian, H., Melillo, J. M., Kicklighter, D. W., McGuire, A. D., Helfrich, J. V. III, Moore, B. III, & VoÈroÈsmarty, C. J. (1998). Effect of interannual climate variability on carbon storage in Amazonian ecosystems. *Nature*, *396*(6712), 664–667. https://doi.org/10.1038/25328

Turner, B. L., Brenes-Arguedas, T., & Condit, R. (2018). Pervasive phosphorus limitation of tree species but not communities in tropical forests. *Nature*, *555*(7696), 367–370. https://doi.org/10.1038/nature25789

Vitousek, P. M., Porder, S., Houlton, B. Z., & Chadwick, O. A. (2010). Terrestrial phosphorus limitation: Mechanisms, implications, and nitrogen-phosphorus interactions. *Ecological Applications*, *20*(1), 5–15. https://doi.org/10.1890/08-0127.1

Walker, T., & Syers, J. (1976). The fate of phosphorus during pedogenesis. *Geoderma*, *15*(1), 1–19. https://doi.org/10.1016/0016-7061(76)90066-5

Wang, Y.-P., Law, R. M., & Pak, B. (2010). A global model of carbon, nitrogen and phosphorus cycles for the terrestrial biosphere. *Biogeosciences*, *7*(7), 2261–2282. https://doi.org/10.5194/bg-7-2261-2010

Wieder, W. R., Cleveland, C. C., Smith, W. K., & Todd-Brown, K. (2015). Future productivity and carbon storage limited by terrestrial nutrient availability. *Nature Geoscience*, *8*(6), 441–444. https://doi.org/10.1038/ngeo2413

Wood, T. E., Cavaleri, M. A., & Reed, S. C. (2012). Tropical forest carbon balance in a warmer world: A critical review spanning microbial-to ecosystem-scale processes. *Biological Reviews*, *87*(4), 912–927. https://doi.org/10.1111/j.1469-185X.2012.00232.x

Wright, S. J., Turner, B. L., Yavitt, J. B., Harms, K. E., Kaspari, M., Tanner, E. V., et al. (2018). Plant responses to fertilization experiments in lowland, species-rich, tropical forests. *Ecology*, *99*(5), 1129–1138. https://doi.org/10.1002/ecy.2193

Wright, S. J., Yavitt, J. B., Wurzburger, N., Turner, B. L., Tanner, E. V., Sayer, E. J., et al. (2011). Potassium, phosphorus, or nitrogen limit root allocation, tree growth, or litter production in a lowland tropical forest. *Ecology*, *92*(8), 1616–1625. https://doi.org/10.1890/10-1558.1

Yang, X., & Post, W. (2011). Phosphorus transformations as a function of pedogenesis: A synthesis of soil phosphorus data using Hedley fractionation method. *Biogeosciences*, *8*(10), 2907–2916. https://doi.org/10.5194/bg-8-2907-2011

Yang, X., Thornton, P., Ricciuto, D., & Post, W. (2014). The role of phosphorus dynamics in tropical forests—A modeling study using CLM-CNP. *Biogeosciences*, *11*(6), 1667–1681. https://doi.org/10.5194/bg-11-1667-2014

Yang, X., Thornton, P. E., Ricciuto, D. M., & Hoffman, F. M. (2016). Phosphorus feedbacks constraining tropical ecosystem responses to changes in atmospheric CO_2 and climate. *Geophysical Research Letters*, *43*, 7205–7214. https://doi.org/10.1002/2016GL069241

Zhang, K., de Almeida Castanho, A. D., Galbraith, D. R., Moghim, S., Levine, N. M., Bras, R. L., et al. (2015). The fate of Amazonian ecosystems over the coming century arising from changes in climate, atmospheric CO_2, and land use. *Global Change Biology*, *21*(7), 2569-2587. https://doi.org/10.1111/gcb.12903